Semianalytical study of the propagation of an ultrastrong femtosecond laser pulse in a plasma with ultrarelativistic electron jitter

Dušan Jovanović, Renato Fedele, Milivoj Belić, and Sergio De Nicola

Citation: Physics of Plasmas **22**, 043110 (2015); doi: 10.1063/1.4916909
View online: http://dx.doi.org/10.1063/1.4916909
View Table of Contents: http://scitation.aip.org/content/aip/journal/pop/22/4?ver=pdfcov
Published by the AIP Publishing

Semianalytical study of the propagation of an ultrastrong femtosecond laser pulse in a plasma with ultrarelativistic electron jitter

Dušan Jovanović,[1,a)] Renato Fedele,[2,3,b)] Milivoj Belić,[4,c)] and Sergio De Nicola[5,d)]
[1]*Institute of Physics, University of Belgrade, Pregrevica 118, 11080 Belgrade, Zemun, Serbia*
[2]*Dipartimento di Fisica, Università di Napoli "Federico II," M.S. Angelo, Napoli, Italy*
[3]*INFN Sezione di Napoli, Complesso Universitario di M.S. Angelo, Napoli, Italy*
[4]*Texas A&M University at Qatar, P.O. Box 23874, Doha, Qatar*
[5]*SPIN-CNR, Complesso Universitario di M.S. Angelo, Napoli, Italy*

(Received 4 February 2015; accepted 23 March 2015; published online 10 April 2015)

The interaction of a multi-petawatt, pancake-shaped laser pulse with an unmagnetized plasma is studied analytically and numerically in a regime with ultrarelativistic electron jitter velocities, in which the plasma electrons are almost completely expelled from the pulse region. The study is applied to a laser wakefield acceleration scheme with specifications that may be available in the next generation of Ti:Sa lasers and with the use of recently developed pulse compression techniques. A set of novel nonlinear equations is derived using a three-timescale description, with an intermediate timescale associated with the nonlinear phase of the electromagnetic wave and with the spatial bending of its wave front. They describe, on an equal footing, both the strong and the moderate laser intensity regimes, pertinent to the core and to the edges of the pulse. These have fundamentally different dispersive properties since in the core the electrons are almost completely expelled by a very strong ponderomotive force, and the electromagnetic wave packet is imbedded in a vacuum channel, thus having (almost) linear properties. Conversely, at the pulse edges, the laser amplitude is smaller, and the wave is weakly nonlinear and dispersive. New nonlinear terms in the wave equation, introduced by the nonlinear phase, describe without the violation of imposed scaling laws a smooth transition to a nondispersive electromagnetic wave at very large intensities and a simultaneous saturation of the (initially cubic) nonlocal nonlinearity. The temporal evolution of the laser pulse is studied both analytically and by numerically solving the model equations in a two-dimensional geometry, with the spot diameter presently used in some laser acceleration experiments. The most stable initial pulse length is estimated to exceed $\gtrsim 1.5$–$2\ \mu$m. Moderate stretching of the pulse in the direction of propagation is observed, followed by the development of a vacuum channel and of a very large electrostatic wake potential, as well as by the bending of the laser wave front. © *2015 AIP Publishing LLC*. [http://dx.doi.org/10.1063/1.4916909]

I. INTRODUCTION

A theoretical investigation of the interaction of an ultrastrong and ultra-short laser pulse with unmagnetized plasma is carried out, aimed for the advancement of the laser wakefield acceleration scheme.[1–4] The study is applied to the specifications planned for the near future and envisaged for the next generation of powerful Ti:Sa lasers. The analysis is based on the Lorentz-Maxwell fluid model in the fully relativistic regime taking the pancake approximation, developed earlier. In our recent paper,[5] we studied in detail only the Weak Intensity Regime (WIR) and Moderate Intensity Regime (MIR), defined at the end of Sec. II. The Strong Intensity Regime (SIR) was discussed in Ref. 5 only qualitatively, and it was pointed out that it was fundamentally different from MIR, since it involved vastly different scalings in the core and at the edges of such pulse. Namely, the electrons are almost completely expelled from the core by a very strong ponderomotive force, creating a *vacuum channel*. An electromagnetic wave packet is imbedded in such vacuum channel and features (almost) linear properties, as if it was propagating in vacuum. Conversely, the edges of the pulse (most importantly, the leading edge) operate within the MIR, and the sort of nonlinear self-organization described in Ref. 5 is expected to occur there. Thus, in order to study the propagation of a very large amplitude pulse, we need a general description that includes both the (quasi)linear behavior inside the vacuum channel and the proper boundary conditions at its edges, including the creation of such vacuum channel by the electron expulsion at the leading edge of the pulse. In this paper, we consider the SIR laser intensities of the order of $I \sim 10^{20}\ \mathrm{W/cm^2}$, which are 30–50 times bigger than those attainable nowadays. With the currently available laser energies, the maximum electron beam energy reached in laser-plasma accelerators (LPAs) is $\gtrsim 1$ GeV,[6] and a fundamental limitation to reach higher beam energies is set by the pump depletion. A simple arithmetics shows that to produce a 10 GeV electron bunch with a charge of 1 nC, holding 10 J of kinetic energy, with a laser to particle beam efficiency 1%–10%, laser energy of 100–1000 J is needed, i.e., $P = 40$–400 PW, if the pulse duration is ~ 25 fs. Most powerful LPA systems at present time, or planned for the near

a)Electronic mail: dusan.jovanovic@ipb.ac.rs
b)Electronic mail: renato.fedele@na.infn.it
c)Electronic mail: milivoj.belic@qatar.tamu.edu
d)Electronic mail: sergio.denicola@spin.cnr.it

future,[7] include the Nd:Glass lasers with the wavelength $\lambda = 1.06\,\mu$m, pulse duration $T = 300$–500 fs and power $P \lesssim 1$ PW, and the facilities using Ti:Sapphire technology, $\lambda = 0.65$–$1.1\,\mu$m, having shorter pulses, $T = 25$–60 fs, and the power $P = 0.1$–1 PW. For example, one of the most powerful laser accelerator devices under way, the Plasmon-X in Frascati, uses the Ti:Sa Frascati Laser for Acceleration and Multidisciplinary Experiments (FLAME), whose characteristics are $E = 7$ J, $\tau \geq 25$ fs, $W \leq 300$ TW, $\lambda = 0.8\,\mu$m, (which corresponds to $\omega = 2.35619 \times 10^{15}\,\mathrm{s}^{-1}$), and $\nu_{rep} = 10$ Hz (repetition frequency). Its pulse duration $T = 25 \times 10^{-15}$ s corresponds to the pulse length $L_z = 7.5\,\mu$m, i.e., there are around 10 wavelengths of laser light within the pulse. Lasers with considerably bigger energies have been planned, mostly in the Nd:Glass technology. The Vulcan upgrade[8,9] will have a new laser beamline with 300 J in 30 fs (10 PW) that can be focused to 10^{23} W/cm^2. Extreme Light Infrastructure (ELI)[10] will produce in its second section, planned for a later phase, a 10 PW beamline compressed to 130 fs, providing an on-target power density $I > 10^{23}$ W/cm^2. The electron acceleration to 2–5 GeV is expected to be reached by 2019 and up to 50 GeV after 2020. Ultra-strong Ti:Sapphire lasers have also been planned, such as Astra-Gemini,[8] a dual beam upgrade to a PW class of the existing Astra facility that will supply 10^{22} W/cm^2 on target. Each beam will have 15 J compressed to 30 fs, supplying 0.5 PW. Further compression to ~5 fs (~2 oscillations) is possible by the use of photon deceleration or thin plasma lenses,[11,12] and the transverse filamentation can be stabilized by a periodic plasma-vacuum structure.[13]

To enable predictions for the multi-petawatt laser pulse behavior, we derive a novel mathematical model that describes both the moderate and the strong intensity regimes. In the classical picture of a slowly varying amplitude of the laser pulse, based on a two-timescale description, this is not possible because the dispersion characteristics of electromagnetic waves in MIR and SIR are too different from each other and cannot be described on a common footing. In the core of a very strong (i.e., SIR) pulse, the electromagnetic wave practically propagates in a vacuum. Such wave is not dispersive, i.e., its group velocity is constant and coincides with its phase velocity. Conversely, at the edges of such pulse, the amplitude is smaller and the wave is dispersive. Under such conditions, the simple envelope description used previously in the MIR breaks down.[14] Our model is derived using a three-timescale description, with an intermediate timescale associated with the nonlinear, intensity-dependent, phase of the electromagnetic pulse. The Schrödinger equation for the phase is considerably simplified under the physical conditions of the FLAME laser system (such as the laser frequency, pulse duration and spot size, and plasma density). For a laser power of order 10^{20} W/cm^2, our equation for the phase can be solved within the Wentzel–Kramers–Brillouin (WKB) approximation. The nonlinear terms in the wave equation coming from the nonlinear phase describe a smooth transition to a nondispersive electromagnetic wave at very large intensities and the saturation of the (initially cubic) nonlocal nonlinearity, without the violation of the imposed scaling laws. These equations are solved numerically in a two-dimensional (2D) geometry. A violent stretching of the laser pulse in the direction of propagation is observed, which permits the pulse to propagate through plasma up to a several mm distance, which is consistent with the conditions of the self-injection experiment.[15,16] The stretching is attributed to nonlocality effects that give rise to an effective mixing of the core of the pulse, propagating with the speed of light through a self-generated vacuum channel, with the front edge of the pulse (which tends to propagate with the group velocity).

II. MATHEMATICAL MODEL

The analytic studies of the laser-plasma interaction with intensities suitable for LPA have been attempted hitherto only for quasi-1D, pancake-shaped pulses, using the "quasistatic" approximation and in a cold-fluid description, see the classical papers[17–20] and references therein. Recently, in the *mildly relativistic regime*, the evolution of the plasma wake and of the laser pulse (depletion, frequency redshifting) was satisfactorily described using a reduced wave equation and a quasistatic plasma response,[21] with a good agreement with full Maxwell-fluid results. Such fluid calculations provide a valuable insight also into kinetic phenomena, e.g., by establishing the thresholds for the wave breaking that results in the electron trapping. Following these works, considering an unmagnetized plasma, assuming $\nabla_\perp \ll \partial/\partial z$, and taking that the solution is slowly varying in the frame that moves with the velocity $u\,\vec{e}_z$, we have derived our system *wave equation + Poisson's equation*, (16), (17). We briefly outline the derivation of such coupled system that involves fully relativistic electrons and the details can be seen, e.g., in our recent paper.[5] We note that Eqs. (16) and (17) are valid also for *ultrarelativistic* electrons, $p_{\perp_0} \gg m_0 c$. Being affected by the return electron current, the wake is inherently electromagnetic, but for sufficiently broad pulses, both pancake-shaped[5,21] and spherical,[22] the electromagnetic effects are weak and the wake may be considered as purely electrostatic. These equations are valid in an unmagnetized plasma, for a solution that is slowly varying in the reference frame moving with the velocity $u\,\vec{e}_z$. They are written in the following dimensionless quantities

$$t' = \omega_{pe} t, \quad \vec{r}\,' = \frac{\omega_{pe}}{c}(\vec{r} - \vec{e}_z\, ut), \quad n' = \frac{n}{n_0}, \quad u' = \frac{u}{c},$$
$$\vec{p}\,' = \frac{\vec{p}}{m_0 c}, \quad \vec{v}\,' = \frac{\vec{v}}{c}, \quad \phi' = \frac{q\phi}{m_0 c^2}, \quad \vec{A}\,' = \frac{q\vec{A}}{m_0 c}, \tag{1}$$

where ω_{pe} is the electron plasma frequency of the unperturbed plasma, $\omega_{pe} = (n_0 q^2/m_0\epsilon_0)^{\frac{1}{2}}$, while $-e$ and m_0 are the electron charge and the rest mass. For simplicity, the primes will be omitted in the rest of the paper. The components of the Maxwell's equations that are parallel and perpendicular to the direction of the e.m. wave propagation (i.e., the wave equation for the perpendicular component of the vector potential, $\vec{A}_\perp$, and the Poisson's equation for the electrostatic potential ϕ) are

$$\left[\frac{\partial^2}{\partial t^2} - 2u\,\frac{\partial^2}{\partial z\,\partial t} - (1-u^2)\frac{\partial^2}{\partial z^2} - \nabla_\perp^2\right]\vec{A}_\perp + \nabla_\perp\left(\frac{\partial}{\partial t} - u\,\frac{\partial}{\partial z}\right)\phi = \vec{v}_\perp n, \tag{2}$$

$$\left(\nabla_\perp^2 + \frac{\partial^2}{\partial z^2}\right)\phi = 1 - n. \tag{3}$$

The electron continuity, the longitudinal and the perpendicular component of the momentum equations are

$$\left(\frac{\partial}{\partial t} - u\,\frac{\partial}{\partial z}\right)n + \nabla\cdot(n\vec{v}) = 0, \tag{4}$$

$$\left(\frac{\partial}{\partial t} - u\,\frac{\partial}{\partial z} + \vec{v}_\perp\cdot\nabla_\perp\right)(p_z + A_z) - \vec{v}_\perp\,\frac{\partial}{\partial z}\left(\vec{p}_\perp + \vec{A}_\perp\right) + \frac{\partial}{\partial z}(\gamma+\phi) = 0, \tag{5}$$

$$\left[\frac{\partial}{\partial t} + (v_z - u)\frac{\partial}{\partial z} + \vec{v}_\perp\cdot\nabla_\perp\right]\left(\vec{p}_\perp + \vec{A}_\perp\right) - v_i\nabla_\perp(p_i + A_i) + \nabla_\perp(\gamma+\phi) = 0, \tag{6}$$

where γ is the relativistic factor, $\gamma = (1+\vec{p}^{\,2}/m_0^2c^2)^{\frac{1}{2}}$, and c is the speed of light.

The solution of the hydrodynamic equations (4)–(6) is sought in a *quasistatic regime*, i.e., when it is slowly varying in the moving reference frame, $\partial/\partial t \ll u\,\partial/\partial z$. However, the hydrodynamic equations (4)–(6) still remain rather complicated, and following the classical works,[18,19,23,24] we further simplify them by adopting u to be very close to the speed of light $0 < 1-u \ll 1$. In Ref. 5, we generalized the results of Refs. 18, 19, 23, and 24 to a 3D geometry, but assuming a *pancake* (i.e., almost one dimensional, 1D) solution, viz., $\nabla_\perp \ll \partial/\partial z$. In the approximate expressions for the charge and current densities, we use the leading order solution of the electron hydrodynamic equations (4)–(6), which is found as a stationary 1D solution that propagates with the speed of light, setting $\partial/\partial t = \nabla_\perp = 1-u = 0$. Then, the leading parts of Eqs. (4)–(6) are obtained in a simple form

$$\frac{\partial}{\partial z}[(v_z-1)n] = 0, \tag{7}$$

$$\frac{\partial}{\partial z}(-p_z + \gamma + \phi) = 0, \tag{8}$$

$$\frac{\partial}{\partial z}\left(\vec{p}_\perp + \vec{A}_\perp\right) = 0, \tag{9}$$

while from $\nabla\cdot\vec{A} = 0$, within the same accuracy, we have

$$\partial A_z/\partial z = 0. \tag{10}$$

Noting that for $z \to \pm\infty$, we have $\phi = \vec{A} = \vec{v} = \vec{p} = 0$ and $\gamma = n = 1$, and using $\gamma = (1 + p_z^2 + \vec{p}_\perp{}^2)^{\frac{1}{2}}$, Eqs. (7)–(10) are readily integrated, yielding

$$(v_z - 1)n + 1 = 0, \tag{11}$$

$$-p_z + \gamma - 1 + \phi = 0, \tag{12}$$

$$\vec{p}_\perp + \vec{A}_\perp = 0, \tag{13}$$

$$A_z = 0. \tag{14}$$

Then, making use of Eqs. (11)–(13) and of the definition of γ, we get dimensionless charge and current densities

$$n = \frac{(\phi-1)^2 + \vec{A}_\perp{}^2 + 1}{2(\phi-1)^2}, \quad \vec{v}_\perp n = \frac{\vec{A}_\perp}{\phi - 1}, \tag{15}$$

which permits us to rewrite our basic equations as

$$\left[\frac{\partial^2}{\partial t^2} - 2u\,\frac{\partial^2}{\partial t\,\partial z} - (1-u^2)\frac{\partial^2}{\partial z^2} - \nabla_\perp^2 + \frac{1}{1-\phi}\right]\vec{A}_\perp = -\left(\frac{\partial}{\partial t} - u\,\frac{\partial}{\partial z}\right)\nabla_\perp\phi, \tag{16}$$

$$\frac{\partial^2\phi}{\partial z^2} = \frac{(\phi-1)^2 - 1 - \vec{A}_\perp{}^2}{2(\phi-1)^2}. \tag{17}$$

The above Eqs. (16) and (17) constitute a system of coupled nonlinear equations that describe the spatio-temporal evolution of an electromagnetic wave, modulated in the form of a pancake, interacting with a Langmuire wave via the nonlocal nonlinearities that arise from the relativistic effects, beyond the slowly varying amplitude approximation and for an arbitrary intensity regime. They appropriately describe all the parametric processes involved, i.e., besides the standard nonrelativistic three-wave coupling (the Raman scattering), they provide also the description of the four-wave processes in a relativistic plasma, directly related to the modulational instability, the soliton formation, etc.

The scaling analysis of Eqs. (16) and (17) indicates that three fundamentally different regimes of operation can be distinguished with respect to the magnitude of the nonlinear term. These are the WIR, $\vec{A}_\perp^2 \ll \epsilon^2 \ll 1$, MIR, $\vec{A}_\perp^2 \sim \epsilon^2$, and SIR, $\vec{A}_\perp^2 \sim 1$. The small parameter ϵ is defined as $\epsilon = \omega_{pe}/\omega$, which under the conditions of the FLAME laser wakefield experiments has the value $\epsilon \approx 1/12$. The dimensionless laser intensity $\vec{A}_\perp^2$ is expressed via the laser parameters as $\vec{A}_\perp^2 = \frac{I}{c^2\epsilon_0}\frac{\lambda^2}{4\pi^2 c}\left(\frac{e}{m_0 c}\right)^2$. Here, λ and I are the laser wavelength and the intensity, $I = 4W/L_\perp^2\pi$, while W is the laser power and $L_\perp$ is the diameter of the spot. The corresponding laser intensities are:

(i) WIR, with the maximum intensity I_{max} ranging from 2.5×10^{14} to 2.5×10^{16} W/cm^2,[25–27] when the electron quiver motion is *weakly relativistic*, $p_{\perp_0} \ll m_0 c$ (here, $p_{\perp_0} = eE_{\perp_0}/\omega$ and ω and $E_{\perp_0}$ are the angular frequency and the amplitude of the laser electric field).

(ii) MIR, with I_{max} ranging from 1.5×10^{18} to 3×10^{19} W/cm^2,[27,28] when the electron quiver motion is *mildly relativistic*, $p_{\perp_0} \lesssim m_0 c$.

(iii) SIR, with I_{max} ranging from 10^{20} to 2.5×10^{22} W/cm^2,[27,29,30] when the electron quiver motion is *ultrarelativistic*, $p_{\perp_0} \gg m_0 c$.

Simple scaling[5] reveals that in the SIR, the electron density perturbation is comparable to the plasma density, i.e., that the ponderomotive force entirely routs plasma electrons from the pulse area and leaves a wake of immobile, positively charged ions. For a spheroidal laser pulse, whose length and width are comparable to the plasma length, $L_\parallel \sim L_\perp \sim 2\pi c/\omega_{pe}$, the threshold for the complete expulsion of the electrons was estimated to be $p_{\perp_0} \geq 4\, m_0 c$.[31] The phenomenological theory[32] has found that such plasma cavity, or *bubble*, develops instead of a periodic plasma wave when the nonlinearities are sufficiently strong to produce a plasma wave breaking after the first oscillation. Three-dimensional particle-in-cell (PIC) simulations[33] confirmed the existence of the *bubble* (also called *the blowout*) regime in LPA and showed that a bubble can trap background electrons and accelerate them, with a monoenergetic spectrum. Spheroidal bubbles are inherently electromagnetic,[34] since the wake is encircled by the return current of relativistic electrons, exerting a Lorentz force on electrons. The balance of the Lorentz, Coulomb, and ponderomotive forces determines the size of a 3D bubble. For self-similar 3D pulses, the optimum wake generation[35,36] occurs for the pulse length $L_\parallel \leq d_s/2$ and the laser spot diameter $d_s = (2c/\omega_{pe})\sqrt{eE_{\perp_0}/\omega m_0 c}$. Due to its inherent complexity, at present time, no reliable analytic analyses of the laser-plasma interaction in the bubble regime have been presented in the literature, and all studies rely solely on the massive PIC numerical simulations. However, in the near future, a regime with a similar laser intensity, for which an analytical or semi analytic treatment will be possible, is expected be realized also in the "pancake" geometry. With the presently available laser energies, a strong intensity pancake pulses would require a simultaneous reduction of both the spot diameter and the pulse length by the modest factor of ~3. Such reduction of the pulse duration to $T \lesssim 10 \times 10^{-15}$ s, which corresponds to the pulse length of mere 3–4 laser wavelengths, i.e., $L_z \lesssim 3\ \mu$m, might be achieved using various techniques, such as the transition through periodic plasma-vacuum structures and plasma lenses,[12,13] self-focusing by the plasma wake[11,37,38] or nonuniform Ohmic heating by the laser pulse, see Ref. 39 and references therein. Together with a slight reduction of the spot diameter, readily available at present time, this would bring us to the verge of the SIR, but still retaining the pancake form of the pulse. Conversely, it is reasonable to expect that in the foreseeable future, the laser energy can be increased 50–100 times, to the level that enables experiments in a strong intensity regime also with presently available pulse lengths. It has been argued[14] that, although PIC algorithms are now getting very fast, fluid models for the plasma response may still be useful. Namely, the simulations of the next generation of LPA experiments (meter-scale, 10 GeV) will increase the computational requirements around 1000-fold, to levels that are almost unattainable. LPA simulations can be vastly improved if one uses the ponderomotive guiding center averaging technique and studies the evolution of the envelope of the laser field, rather than the field itself,[40] but such procedure breaks down for very intense pump strengths.[14] In this paper, we develop a method to avoid such breakdown, using a three-timescale procedure described in the Subsections III A–III D.

III. WAVE MODULATION AND THE SCALING LAWS

A. Beyond the modulational representation. Nonlinear phase evolution on intermediate scale

For both moderate (MIR) and strong intensities (SIR), we seek the solution of the wave equation in the moving frame (2) as the sum of a slowly varying component and a modulated electromagnetic wave, including a phase φ that is varying on an intermediate scale, viz.

$$\vec{A}_\perp = \vec{A}_\perp^{(0)}(t_2, \vec{r}_2) + \{\vec{A}_{\perp_0}(t_2, \vec{r}_2)\ e^{i[\varphi(t_1,\vec{r}_1) - \omega' t + k'(z+ut)]} + c.c.\}. \quad (18)$$

The slowly varying vector potential $\vec{A}_\perp^{(0)}(t_2, \vec{r}_2)$ corresponds to the self-generated quasistationary magnetic field. The dimensionless frequency ω' and wavenumber k' of the rapidly varying part of the vector potential are

$$\omega' = \frac{\omega}{\omega_{pe}}, \quad k' = \frac{ck}{\omega_{pe}} = \frac{d_e}{\lambda}, \quad (19)$$

while ω, k, and λ are, respectively, the frequency, the wavenumber, and the wavelength of the electromagnetic wave propagating in an unperturbed plasma that satisfy the linear dispersion relation $\omega = \sqrt{c^2k^2 + \omega_{pe}^2}$. For simplicity, hereafter, we drop the primes and write the dimensionless version of the dispersion relation as

$$\omega = \sqrt{k^2 + 1}. \quad (20)$$

The quantity $\epsilon \equiv 1/\omega \ll 1$ is a small parameter. For example, under the conditions of the FLAME laser-plasma experiments, we have $\omega \approx k \gtrsim 12$. Likewise, the spatial derivative in the direction of propagation is estimated as $\partial \vec{A}_{\perp_0}/\partial z \sim \vec{A}_{\perp_0}/L_\parallel$, where $L_\parallel = c\,T = 7.5\ \mu$m is the pulse length and T is the pulse duration. The dimensionless value of the pulse length, see Eq. (1), is then $L'_\parallel = T\omega_{pe} = 4.46$. The intermediate and slow timescales, introduced in Eq. (18) and denoted by the subscripts 1 and 2, respectively, are given by

$$t_1 = \epsilon\, t - \epsilon^{-1} uz, \quad \vec{r}_1 = \vec{e}_x x + \vec{e}_y y + \epsilon^{-1}\vec{e}_z z,$$
$$t_2 = \epsilon^2 t_1 = \epsilon^3 t - \epsilon\, uz, \quad \vec{r}_2 = \epsilon\,\vec{r}_1 = \epsilon(\vec{e}_x x + \vec{e}_y y) + \vec{e}_z z, \quad (21)$$

while the nonlinear phase $\varphi(t_1, \vec{r}_1)$ will be conveniently introduced later. We adopt u to be equal to the group velocity of an electromagnetic wave

$$u = d\omega/dk = k/\omega, \quad (22)$$

which permits us to rewrite the wave equation (16) and the Poisson's equation (17) as

$$2\,\mathrm{Re}\left\{e^{i\left[\varphi(t_1,\vec{r}_1)-t/\omega+kz\right]}\left[\alpha\vec{A}_{\perp_0}-2i\epsilon^2\left(1-\frac{\partial\varphi}{\partial t_1}\right)\frac{\partial\vec{A}_{\perp_0}}{\partial t_2}\right.\right.$$
$$\left.\left.-2i\epsilon(\nabla_1\varphi\cdot\nabla_2)\vec{A}_{\perp_0}+\epsilon^4\frac{\partial^2\vec{A}_{\perp_0}}{\partial t_2^2}-\epsilon^2\nabla_2^2\vec{A}_{\perp_0}\right]\right\}$$
$$=\epsilon\left(\epsilon\frac{\partial}{\partial t_2}-u\frac{\partial}{\partial z_2}\right)\nabla_{2\perp}\phi-\left(\epsilon^4\frac{\partial^2}{\partial t_2^2}-\epsilon^2\nabla_2^2-\frac{1}{1-\phi}\right)\vec{A}_\perp^{(0)},\tag{23}$$

$$\left(\frac{\partial}{\partial z_2}-\epsilon u\frac{\partial}{\partial t_2}\right)^2\phi=\frac{(\phi-1)^2-1-\vec{A}_\perp{}^2}{2(\phi-1)^2},\tag{24}$$

where $\vec{A}_\perp{}^2$ stands for $\vec{A}_\perp\cdot\vec{A}_\perp$ and

$$\alpha=(\nabla_1\varphi)^2-i\nabla_1^2\varphi+2\frac{\partial\varphi}{\partial t_1}-\left(\frac{\partial\varphi}{\partial t_1}\right)^2+i\frac{\partial^2\varphi}{\partial t_1^2}+\frac{\phi}{1-\phi},\tag{25}$$

while $\nabla_k=\vec{e}_x(\partial/\partial x_k)+\vec{e}_y(\partial/\partial y_k)+\vec{e}_z(\partial/\partial z_k)$, $k=1,\ 2$. The right-hand-side of the wave equation (23) is slowly varying in space and time, and, for that reason, it is not resonant with the high-frequency oscillations of the vector potential on the left-hand-side. The slow component of the vector potential, $A_\perp^{(0)}$, is related with the quasistationary magnetic field generated in the laser-plasma interaction, for whose accurate description it would be necessary to include also the kinetic effect that are responsible, e.g., for the off-diagonal terms in the stress tensor for electrons,[27,41] and for the return electron current.[42–44] For the structure of the magnetic field created in the Weibel instability of the return current see, e.g., Ref. 45 and references therein. However, to be consistent with the derivation used in this paper which is based on a cold and unmagnetized plasma model, we have to restrict our analysis to the regime when the right-hand side of Eq. (23) is negligible.

B. Nonlinear phase

First, we adopt the phase φ to be a nonlinear function of the wake potential ϕ, satisfying the equation

$$\alpha-\frac{\phi}{1-\phi}+i\left(\nabla_1^2\varphi-\frac{\partial^2\varphi}{\partial t_1^2}\right)$$
$$=(\nabla_1\varphi)^2+2\frac{\partial\varphi}{\partial t_1}-\left(\frac{\partial\varphi}{\partial t_1}\right)^2\equiv\kappa^2(\phi),\tag{26}$$

where $\kappa(\phi)$ is a localized, well-behaved function of its argument that will be conveniently adopted later. With such choice of κ, the right-hand-side of Eq. (26) is varying on the same temporal and spatial scales as the wake potential $\phi(t_2,\vec{r}_2)$, see Eqs. (17) and (24), i.e., we have the scaling $\kappa^2(\phi)\sim(t_2,\vec{r}_2)=(\epsilon^2t_1,\epsilon\vec{r}_1)$. In other words, the function $\kappa^2(\phi)$ is adopted to be a slowly varying function of the spatial variables $\vec{r}_1$ and a *very slowly* varying function of the temporal variable t_1. With such choice, the fundamental solution of Eq. (26), which we will use as the nonlinear phase φ in the rest of the paper, is a slowly time-varying function, viz., $\partial\varphi/\partial t_1\ll1$.

To be consistent with the stationary, 1D approximation used in the derivation of the Poisson's equation (17), we need to solve Eq. (26) with the accuracy to ϵ^2. First, we note that it can be considerably simplified if we introduce the following new variables:

$$\vec{\rho}=\vec{r}_1,\qquad\tau=t_1-\int_{-\infty}^{\vec{r}_1}\frac{\vec{dl}\cdot\nabla_1\varphi}{(\nabla_1\varphi)^2},\tag{27}$$

yielding $\nabla_1=\nabla_\rho-\nabla_1\varphi(\nabla_1\varphi)^{-2}\,\partial/\partial\tau$, and thus

$$\frac{\partial}{\partial t_1}=\left[1-\frac{\partial}{\partial t_1}\int_{-\infty}^{\vec{r}_1}\frac{\vec{dl}\cdot\nabla_1\varphi}{(\nabla_1\varphi)^2}\right]\frac{\partial}{\partial\tau},\tag{28}$$

where $\nabla_\rho=\vec{e}_j\,(\partial/\partial\rho_j)$. Equation (26) is now simplified, viz.

$$(\nabla_\rho\varphi)^2-\kappa^2(\phi)=\mathcal{O}(\epsilon^4).\tag{29}$$

In Eq. (29), the derivatives with respect to the retarded time τ appear only in the small terms, of order $\mathcal{O}(\epsilon^4)$, and can be neglected. We also note that $\kappa(\phi)$ (which quantitatively describes the nonlinear laser–plasma interaction) is a slowly varying function of the spatial variable $\vec{\rho}$, since $\phi=\phi(\epsilon^2\tau,\epsilon\vec{\rho})$. From a physical reasoning (we will demonstrate this point later), we also intuitively expect that κ^2 is a positive definite function, i.e., that κ does not have any zeros on the $\vec{\rho}$ plane. Rather, it exponentially tends to zero for $|\vec{\rho}|\to\infty$, where it enters the linear regime, in which we have $\partial/\partial\tau\to0$. Thus, the transformation Eq. (27) is well behaved on the entire $\vec{\rho}$ plane. In the 1D case, $\partial A_{\perp_0}/\partial x_2=\partial A_{\perp_0}/\partial y_2=0$, Eq. (29) is readily solved as $\varphi=\int\kappa\,d\zeta$, where $\zeta=\vec{e}_z\cdot\vec{\rho}$, while in 2 and 3 dimensions, it can be solved only numerically and with considerable difficulties. It is reasonable to expect that, in a 3D regime, φ is of a similar order of magnitude as in 1D and, as a consequence, our basic Eqs. (23) and (24) features the following scaling:

$$2\,\mathrm{Re}\left\{e^{i\left[\varphi(t_1,\vec{r}_1)-t/\omega+kz\right]}\left[\alpha\vec{A}_{\perp_0}-2i\epsilon^2\frac{\partial\vec{A}_{\perp_0}}{\partial t_2}\right.\right.$$
$$\left.\left.-2i\epsilon(\nabla_\rho\varphi\cdot\nabla_2)\vec{A}_{\perp_0}-\epsilon^2\nabla_2^2\vec{A}_{\perp_0}+\mathcal{O}(\epsilon^3)\right]\right\}$$
$$=\epsilon\left(\epsilon\frac{\partial}{\partial t_2}-u\frac{\partial}{\partial z_2}\right)\nabla_{2\perp}\phi-\left(\epsilon^4\frac{\partial^2}{\partial t_2^2}-\epsilon^2\nabla_2^2-\frac{1}{1-\phi}\right)\vec{A}_\perp^{(0)},\tag{30}$$

$$\frac{\partial^2\phi}{\partial z_2^2}=\frac{(\phi-1)^2-1-\vec{A}_\perp{}^2}{2(\phi-1)^2}+\mathcal{O}(\epsilon).\tag{31}$$

C. Regime in which the self-generated magnetic field can be neglected

The left-hand-side of the wave equation (23), or (30), describes the evolution of the envelope of the laser pulse, while the right-hand-side, whose characteristic frequency and wavevector are equal to zero, describes the slowly

varying magnetic field created by the laser pulse. However, the latter is not adequately described by our simple hydrodynamic equations (4)–(6) that are based on a cold, unmagnetized plasma model. Within the accuracy with which the nonlinear current and charge densities have been derived, our wave equation (30) is valid only if its right-hand side is negligible. A simple scaling analysis of Eqs. (30) and (31) indicates that in a 3D case ($\nabla_{2\perp} \sim \partial/\partial z_2$), the self-generated magnetic field (i.e., the slowly varying vector potential $\vec{A}_\perp^{(0)}$) can be neglected when

$$\max(\phi, |\vec{A}_{\perp_0}|, |\vec{A}_\perp^{(0)}|) < \epsilon^{-1}. \tag{32}$$

Particularly simple case is that of a circularly polarized wave, $\vec{A}_{\perp_0} = (A_{\perp_0}/\sqrt{2})(\vec{e}_x \pm i\,\vec{e}_y)$, for which we have $\vec{A}_\perp^2 = |A_{\perp_0}|^2$, i.e., the second harmonic is absent. Similarly, for a linearly polarized wave, we will neglect the second harmonic (because its contribution is nonresonant) and use $\vec{A}_\perp^2 \approx |A_{\perp_0}|^2$, where $\vec{A}_{\perp_0} = A_{\perp_0}\,\vec{e}_x$.

Now, with the accuracy to ϵ^2, our basic system of equations reduces to

$$[\alpha_{Re}(\phi) + i\,\alpha_{Im}(\phi)]A_{\perp_0} - 2\,i\,\epsilon^2\,\frac{\partial A_{\perp_0}}{\partial t_2} - 2\,i\,\epsilon(\nabla_\rho\varphi\cdot\nabla_2)A_{\perp_0} - \epsilon^2\,\nabla_2^2 A_{\perp_0} = 0, \tag{33}$$

$$\frac{\partial^2\phi}{\partial z_2^2} = \frac{(\phi-1)^2 - 1 - |A_{\perp_0}|^2}{2(\phi-1)^2}, \tag{34}$$

$$(\nabla_\rho\varphi)^2 = \kappa^2(\phi), \tag{35}$$

where variables $(\tau, \vec{\rho})$ are defined in Eq. (27) and α_{Re} and α_{Im} are the real and imaginary parts of α, respectively

$$\alpha_{Re}(\phi) = \phi/(1-\phi) + \kappa^2(\phi),$$
$$\alpha_{Im}(\phi) = -\nabla_1^2\varphi + \frac{\partial^2\varphi}{\partial t_1^2} = -\nabla_\rho^2\varphi + \mathcal{O}(\epsilon^4). \tag{36}$$

The spatial integral of the laser pulse intensity is conserved. Multiplying Eq. (33) by $A_{\perp_0}^*$, taking the imaginary part and integrating for the whole space, we have

$$\frac{\partial}{\partial t_2}\int d^3\vec{r}_2\,|A_{\perp_0}|^2 = \int d^3\vec{r}_2\,|A_{\perp_0}|^2\left[\epsilon^{-1}\,\nabla_2\cdot\nabla_\rho\varphi + \epsilon^{-2}\,\alpha_{Im}(\phi)\right] = \mathcal{O}(\epsilon^2), \tag{37}$$

which is negligible within the adopted accuracy.

D. Model for the nonlinear terms $\alpha_{Re}(\phi)$ and $\kappa(\phi)$

The simplest choice for the function κ and the corresponding expression for α_{Re} [see Eq. (36)], that provide a proper asymptotic ordering of the wave equation for both $\phi \ll 1$ and $\phi \gg 1$, are given by the standard focusing-defocusing model for the *nonlinearity function* $\alpha_{Re}(\phi)$:

$$\alpha_{Re}(\phi) = \frac{\phi}{(1-\phi)^2} \quad \Rightarrow \quad \kappa(\phi) = \frac{-\phi}{1-\phi}, \tag{38}$$

which are displayed in red color in Fig. 1. In the weak and moderate intensity regimes (WIR and MIR), $|\phi| \sim \epsilon^2$, such choice of $\alpha_{Re}(\phi)$ gives the scaling $\alpha_{Re}(\phi) \sim \kappa(\phi) \sim \varphi \sim \mathcal{O}(\epsilon^2)$ and, keeping only the leading terms which are of the order $\mathcal{O}(\epsilon^2)$, our Eqs. (33)–(35) reduce to a Schrödinger equation with a nonlocal cubic nonlinearity, studied in detail in our earlier paper.[5] Conversely, in the SIR, $1 \ll \phi \lesssim 1/\epsilon$ (recall, $\phi \lesssim 1/\epsilon$ is the upper limit for the potential ϕ, when we still may neglect the self-generated magnetic field), we have $\alpha_{Re} \to 1/\phi \to -\epsilon$ and $\kappa \to 1$. Thus, in the SIR and with the accuracy to leading order in ϵ, our basic Eqs. (33)–(35) reduce to a linear equation

$$A_{\perp_0} + 2\,i(\nabla_\rho\varphi\cdot\nabla_2)A_{\perp_0} = 0, \tag{39}$$

where from Eqs. (34) and (35), we have $|\nabla_\rho\varphi| = 1$ and $\phi = -|A_{\perp_0}|$. As discussed earlier, see, e.g., Ref. 5, the above describes a vacuum channel that has been created by a very strong laser pulse. The ponderomotive force associated with such laser pulse is so strong that the electron density perturbation, Eq. (15), is very large, viz., $\delta n = n - 1 \sim \mathcal{O}(1)$, i.e., practically all electrons have been removed and the pulse propagates in vacuum.

Closer to the edges of a SIR laser pulse, in the region where $\phi \sim \mathcal{O}(1)$, the simple choice (38) for the function $\alpha_{Re}(\phi)$ attains a relatively large value, $\alpha_{Re}(-1) = 1/4$. Thus, the nonlinear term $\alpha A_{\perp_0}$ in the wave equation becomes relatively large and it can be balanced by the linear terms only if the space/time variation of the amplitude $A_{\perp_0}(t_2, \vec{r}_2)$ is sufficiently rapid. As a consequence, in the numerical solution of Eqs. (33)–(35) for a SIR laser pulse, there may arise numerical problems (e.g., with convergence, stability) in the spatial region where $\phi \sim \mathcal{O}(1)$, which is a typical value in our numerical examples in Subsections IV A and IV B. Such difficulty may be avoided if we adopt a different functional dependence for $\alpha_{Re}(\phi)$, which features the same asymptotic behavior for $|\phi| \ll 1$ and $|\phi| \gg 1$ as the simplest choice

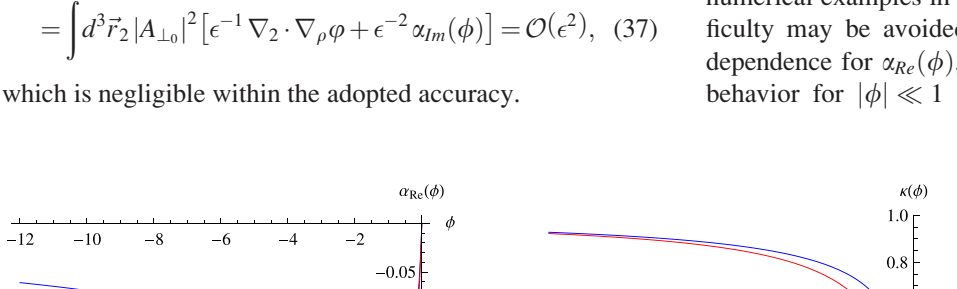

FIG. 1. Left: nonlocality functions $\alpha_{Re}(\phi) = \phi/(1-\phi)^2$ (red line) and $\alpha_{Re}(\phi) = \phi(1+\phi)^2/(1-\phi)^4$ (blue line). Right: functions $\kappa(\phi) = -\phi/(1-\phi)$ (red line) and $\kappa(\phi) = [-\phi/(1-\phi)][1 + 2/(1-\phi)^2]^{1/2}$ (blue line).

Eq. (38), but remains sufficiently small for $|\phi| \sim 1$. There exists a broad range of possible choices for such functions. As a simple example, we propose

$$\alpha_{Re}(\phi) = \frac{\phi(1+\phi^2)}{(1-\phi)^4} \Longleftrightarrow \kappa(\phi) = \frac{-\phi}{1-\phi}\left[1 + \frac{2}{(1-\phi)^2}\right]^{\frac{1}{2}}. \tag{40}$$

These functions are displayed in blue color in Fig. 1. We note that they provide the proper scaling of the wave equation both in the asymptotic regions $\phi \ll 1$ and $\phi \gg 1$, and in the intermediate domain $\phi \sim 1$.

We conclude this section by writing the wave equation in an explicit form, which is possible only in the 1D regime. First, we note that for $\nabla_{2_\perp} \ll \partial/\partial z_2$, the right-hand-side of the wave equation (30) can be neglected for arbitrarily large intensities, i.e., we are not restricted by the condition (32). Next, in the 1D regime, Eq. (29) for the nonlinear phase can be solved as

$$\partial\varphi/\partial\zeta = \kappa(\phi), \tag{41}$$

which after substitution into the wave equation (33) gives

$$\left[\alpha_{Re}(\phi) - i\epsilon\,\frac{\partial\kappa(\phi)}{\partial z_2}\right]A_{\perp_0} - 2\,i\,\epsilon^2\,\frac{\partial A_{\perp_0}}{\partial t_2} - 2\,i\,\epsilon\,\kappa(\phi)\frac{\partial A_{\perp_0}}{\partial z_2} - \epsilon^2\,\frac{\partial^2 A_{\perp_0}}{\partial z_2^2} = 0, \tag{42}$$

where the electrostatic potential ϕ is found from the Poisson's equation (34), while for the functions $\kappa(\phi)$ and $\alpha_{Re}(\phi)$, we may use either the expressions (38) or (40).

IV. NUMERICAL SOLUTIONS

To build an efficient LPA, one needs to determine, within the technical constraints of the available (and soon-to-become available) lasers, the system's specifications that optimize its performance. This can be tedious due to the large number of parameters involved (the initial state of the pulse alone is determined by three parameters—phase, length, and amplitude). We start by making an "educated guess" about the most stable length of the laser pulse, based on simple estimates[18] under simplified, albeit unphysical, conditions. Then we test the stability of such solution in 1D, and finally, we fine tune the laser parameters by solving numerically our basic equations under more realistic physical conditions in 2D. The inherent simplicity of our analytic method enables us to obtain a solution on a standard personal computer (PC) and using an "off the shelf," general purpose numerical package.

It can be easily shown that in the local limit, setting $\partial^2\phi/\partial z^2 \to 0$ in the Poisson's equation (17), there exists a simple 1D localized stationary solution of the wave equation (16) for the laser vector potential, whose envelope is traveling with a constant velocity, see Ref. 18. Choosing that its amplitude a_{max} belongs to the strong intensity regime and that the corrections due to the self-generated magnetic field are sufficiently small, e.g., for $a_{max} = 14.12$, we estimate its e-folding length to be $L_{||} \sim 0.65$, which in the physical (non-scaled) variables corresponds to $L_{||} \sim 1.1\,\mu$m. Obviously, for pulse lengths of that order, the effects of nonlocality cannot be neglected. We study the effects of the latter by the numerical solution of Eqs. (33)–(35) and with the function $\alpha_{Re}(\phi)$ in the form Eq. (40).

A. One dimensional results

First, we restricted our study to the 1D regime, $\partial/\partial x_2 = \partial/\partial y_2 = 0$. In a nonlocal Strong Intensity Regime, we found the numerical solution of Eqs. (42) and (33), using the model (40) and (41) for nonlinear phase φ. We used the numerical method of lines with the spatial discretization involving 900 points and 15 000 steps in time. The initial wake potential and nonlinear phase were adopted to be equal to zero, $\phi(z_2, 0) = \varphi(z_2, 0) = 0$, while the initial laser amplitude was taken in the form of a scaled local solution, $A_{\perp_0}(z_2, 0) = a_L(z_2/L_z)\,\exp(i\,\delta k\, z_2)$, where the local solution $a_L(z_2)$[18] is adopted with $a_{max} = 14.12$ and $L_{||} \sim 0.65$.

Even after an extensive search, we were unable to find any stationary nonlocal solutions. The longest lifetime was observed when the initial conditions were close to the local solution, i.e., for $L_z \lesssim 1$, when the temporal evolution could be described as the breakdown of the initial pulse into two pulses propagating with the group velocity of the electromagnetic wave and with the speed of light, respectively. This disintegration was not complete since these "daughter pulses" remained attached to each other via an inclined plateau (ramp). Depending on the characteristic wavenumber δk, different patterns in the redistribution of the intensity $|A_{\perp_0}|$ among the two pulses and the plateau were observed, yielding either to the rapid spatial dispersion of the structure or its dismemberment via the generation of short scales. The longest living structure was that in which the "daughter pulses" were the least prominent, so that the overall picture could be described as the forward stretching of the initial laser pulse into a wedge-shaped structure. As a_L is independent on the characteristic wavenumber δk, the latter is a free parameter and the value $\delta k = -0.5$ was adopted such as to maximize the lifetime of the pulse, which was determined after a large number of numerical tests. Consistent with the SIR in a pancake geometry, we adopted also $C_1 = -19$ and $L_z = 0.8$, which correspond to the initial full e-folding length of the pulse $L_{||ef} = 0.52$ (in physical units $L_{||ef} = 0.9\,\mu$m). The adopted SIR amplitude $|A_{max}| = 14.12$ (in physical units this corresponds to the wave intensity $I = 0.6 \times 10^{20}\,\mathrm{W/cm^2}$) is well within the ultrarelativistic regime determined by $a \geq 4$,[31] and it is 35 times bigger than that we used previously in the MIR study, see Fig. 2 of Ref. 5 (note that a different normalization was used there). Our initial e-folding length is 1/3 of that used in the earlier MIR calculations.[5]

Our 1D SIR solution is displayed in Fig. 2. We were able to follow its evolution until the emergence of short spatial scales at $t_{2_{max}} \gtrsim 1$ (i.e., $t_{2_{max}} \gtrsim 9.69 \times 10^{-12}$ s in physical units), which practically coincides with the plasma interaction length used in the self-injection test experiment (SITE) using FLAME.[15,16] The pulse length (which was unrealistically short at $t_2 = 0$) was rapidly stretched and increased,

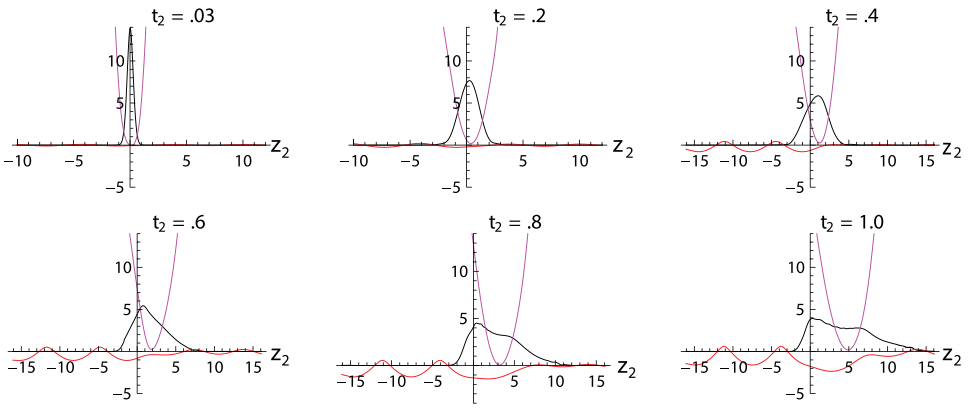

FIG. 2. The forward stretching of a 1D laser pulse in the nonlocal strong intensity regime (with $\partial^2\phi/\partial z_2^2 \neq 0$ and $\nabla_{2\perp}A_{\perp_0} \to 0$). The laser amplitude $|A_{\perp_0}|$ (black), the electrostatic potential ϕ (red), and the phase $\delta\varphi = \arg(A_{\perp_0})$ (magenta) are obtained as the numerical solutions of Eqs. (42) and (33), using the model (40) and (41) for the nonlinear phase φ. The initial condition is adopted in the form of a local solution, $A_{\perp_0}(z_2,0) = a_L(z_2/L_z)\exp(i\,\delta k\, z_2)$, with $\delta k = -0.5$ and $L_z = 0.8$.

eventually, around tenfold. Simultaneously, the peak value of the laser amplitude rapidly dropped from $|A_{max}| \approx 14$ to $|A_{max}| \sim 5$ and remained more-less on that level. The observed temporal evolution was 3–5 times faster than in the MIR case. The electrostatic potential also developed rather rapidly, by the time $t_2 \sim 0.3$, featuring a very large first minimum with $\phi_{max} \sim -2$ and an oscillating, non-sinusoidal, wake. The electrostatic potential was ~200 times bigger than in the MIR case[5] (note a different normalization). Due to the fast stretching of the laser pulse, we observed a vigorous transfiguration of the electrostatic potential ϕ and the emergence of a second parasitic minimum within the pulse. Such fast evolving potential might not be well suited for a particle acceleration.

B. Two dimensional results

The influence of the transverse effects has been studied by the numerical solution of Eqs. (33)–(35) and (40) in the 2D regime $\partial/\partial y_2 = 0$. Because of the violent stretching of a very short laser pulse (~1–2 laser wavelengths) that was observed in the 1D case, studied in Subsection IV A, for a 2D numerical study, we adopt the laser parameters that are both somewhat longer and achievable in a near future. We employed a laser pulse with 60% amplitude and twice the length of the estimate for the local solution,[18] i.e., we used the initial condition (in non-scaled variables) having the r.m.s width $L_{\perp rms} = 150\,\mu$m, the laser energy $E \approx 100$ J, and the power $P \approx 20$ PW. We assumed a

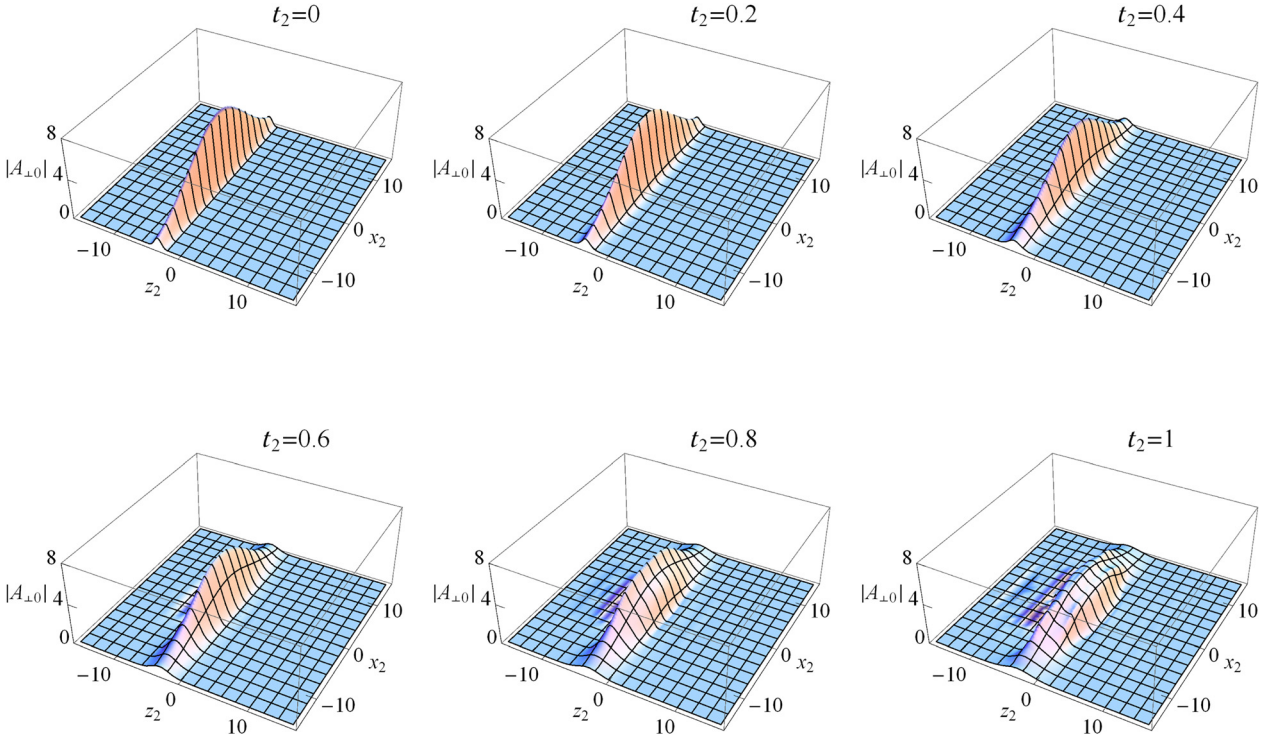

FIG. 3. The evolution, in an ultrarelativistic regime, of the envelope $|A_{\perp_0}(x_2,z_2,t_2)|$ of a pancake laser pulse with an amplitude that is expected to be used in a future accelerator scheme (referred to in the text as a strong intensity regime). The initial condition was similar to that in the 1D case, with a transverse Gaussian profile, the amplitude reduced to 60%, and twice the length in z direction, viz. $A_{\perp_0}(x_2,z_2,0) = 0.6\,a_L(z_2/L_z)\,\exp(-x_2^2/2L_x^2)\exp(i\,\delta k\, z_2)$, with $L_z = 1.6$ and $L_x = 7.5$. We also take $\delta k = 0.5$, which gave the maximum stability. The initial electrostatic potential and initial nonlinear phase were adopted to be zero, $\phi(x_2,z_2,0) = \varphi(x_2,z_2,0) = 0$. In the physical (non-scaled) variables, these initial pulse length and width are 1.8 μm and 300 μm, respectively. Likewise, the dimensionless time $t_{2max} = 1.1$ corresponds, in physical units, to 9.69×10^{-12} s, during which time the pulse travels ~3 mm.

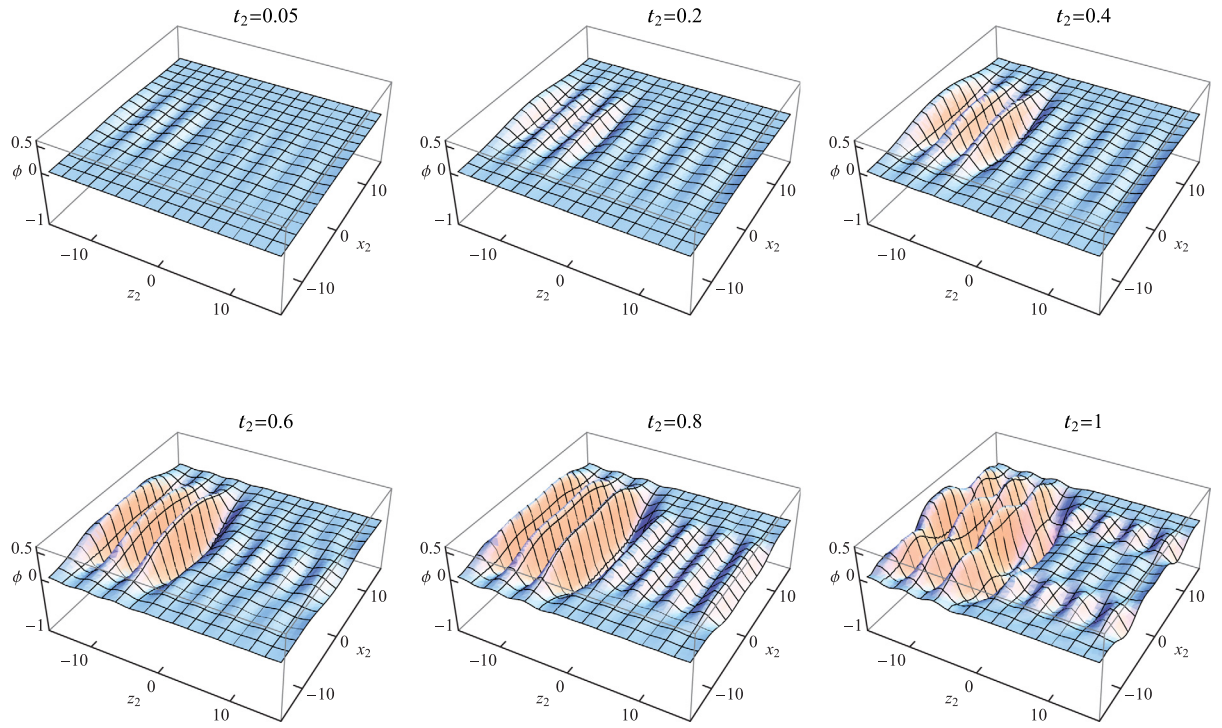

FIG. 4. The evolution of the electrostatic wake potential $\phi(x_2, z_2, t_2)$, produced by the laser pulse displayed in Fig. 3. A very large localized negative potential is created, with $|\phi| \sim 1$, which indicates the almost complete expulsion of electrons in the vicinity of the laser pulse.

Gaussian transverse profile, viz., $A_{\perp_0}(x_2, z_2, 0) = 0.6\, a_L(z_2/L_z) \exp(i\,\delta k\, z_2) \exp(-x_2^2/2L_x^2)$, where a_L the bell shaped, local, stationary solution whose amplitude is $a_{max} = 14.12$, and we adopt $L_x = 7.5$ and $L_z = 1.6$ (i.e., pulse duration $\sim$5.5 ps). After many tests, we found that the most stable evolution is obtained when $\delta k = 0.5$. We consider an initially quiescent plasma $\phi(x_2, z_2, 0) = \varphi(x_2, z_2, 0) = 0$. Our numerical solution was obtained on a standard PC by an "off the shelf" numerical package, based on the method of lines, with a discretization having 64×512 points in the x, z plane and 3000 steps in time. For Eq. (35), we used an iterative procedure. Periodic

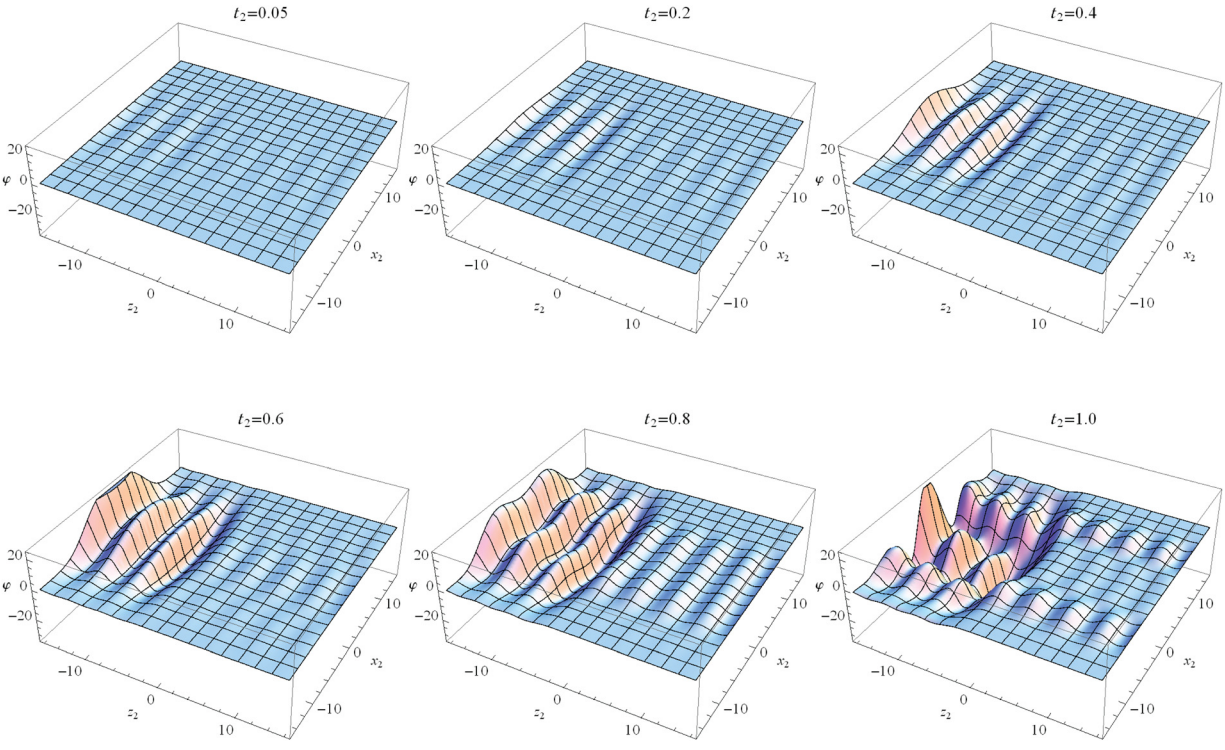

FIG. 5. The evolution of the nonlinear phase $\varphi(x_2, z_2, t_2)$ of the laser pulse displayed in Fig. 3. A noticeable bending of the wave front occurs for $t_2 > 0.5$, simultaneously with the emergence of an electrostatic wake.

boundary conditions were used, with a dissipative layer placed in the front edge of the computational box. Due to the finiteness of such dissipations and the residual coupling between the front and rear edges of the box, an unphysical but rather small signal appeared also in front of the pulse. Our numerical scheme became unstable at $t_{2_{max}} \sim 1.1$ (10^{-11} s in physical units). During this time, pulse traveled 3 mm, similar to the lengths of LPA self-injection experiments and simulations.[15,46] The results are displayed in Figs. 3–5. Neither a transverse contraction nor the folding of the pancake pulse to a V-shape, known in the MIR,[5,20] was observed before the offset of the numerical instability at $t_{2_{max}}$. Due to a stretching in the forward direction, occurring mostly in the central part of the pulse where the amplitude was the largest, the laser amplitude dropped by 40%, to $|A_{max}| \sim 5$, which is still within the ultrarelativistic regime, $|A_{\perp_0}| \geq 4$.[31] By the time $t_{2_{max}}$ the maximum forward stretching (2–3 fold, mostly in the central part) was reached. On the sides of the pulse, a slight stretching took place both in the forward and backward directions, which is attributable to the linear dispersion of the wave packet. Inside the pulse, the electron density was almost zero and the laser light practically propagated in a vacuum, i.e., the core of the pulse propagated with the speed of light and the nonlinear effects were weak. The nonlocality produced an effective mixing with the front edge of the pulse (that tends to propagate with the group velocity), which is pushed forward by the core. Oscillating wake with a large first potential minimum $|\phi_{max}| \sim 1$ developed by $t_2 = 0.5$. The nonlinear phase φ evolved simultaneously with the wake and produced a bending of the laser wave front.

V. CONCLUSIONS

In this paper, we have studied, using a (semi)analytic hydrodynamic description, the strong intensity (also called the *ultrarelativistic*) regime of the propagation of pancake-shaped laser pulses through an unmagnetized plasma, with specifications that are planned to be reached in the next generation of LPA experiments. We have derived nonlinear equations that appropriately describe all three intensity regimes, discussed earlier.[5] In the classical picture of the slowly varying amplitude of a laser pulse, based on a two-timescale description, it is not possible to study the strong- and moderate-intensity regimes simultaneously, because the dispersion characteristics of electromagnetic waves in MIR and SIR are too different from each other and can not be described on a common footing. In the core of a very strong (i.e., SIR) pulse, the electromagnetic wave practically propagates in a vacuum. Such wave is not dispersive, i.e., its group velocity is constant and coincides with its phase velocity. Conversely, at the edges of such pulse, the amplitude is smaller and the wave is dispersive. Under such conditions, the simple envelope description, suitable for the MIR, breaks down.[14] We derive novel model equations, based on a three-timescale description, that account for the evolution of the nonlinear phase of the laser wave. At very large laser intensities, this gives a smooth transition to a nondispersive e.m. wave and the saturation of the nonlocal nonlinearity. These equations are solved numerically, on a standard PC, in the regime when the ultrarelativistic electrons are almost expelled by the radiation pressure of a femtosecond laser pulse focussed to a $\gtrsim 100\,\mu$m spot. We could follow the pulse along a 3 mm path, which is comparable with the plasma dimensions in self-injection experiments and simulations reported in the literature.[15,34,46] The observed temporal evolution was 3–5 times faster than in the MIR case.[5] We have observed, practically, no transverse self-focusing and filamentation for such broad pulse, but its Raleigh length is sufficiently long to allow for an efficient electron acceleration without self-guiding. For the plasma wake, whose peak potential is $|\phi| \sim 1$, the characteristic length has remained close to the plasma length λ_p. The nonlocality effects associated with the plasma wake stretch the laser pulse 2–3 fold in the forward direction. In the *mildly relativistic* (Moderate Intensity) regime, a modest stretching has been observed for pulses that, initially, were sufficiently shorter than the plasma length λ_p.[5,20] Conversely, MIR pulses that are $\gtrsim \lambda_p$ are known to undergo longitudinal compression into a "laser piston."[47] For these, a mild stretching may be desirable,[46] because it compensates the nonlinear red-shift and delays the formation of the "piston," which reduces the dark current. Our calculations have been performed for a laser energy ~ 100 J per pulse with the duration $T \gtrsim 5$ fs, providing the power of several tens of petawatts and the intensity $\sim 10^{20}$ W/cm^2. Our (semi)analytic fluid theory may be a valuable tool for the predictions and the analyses of LPA experiments in the ultrarelativistic regime with these lasers, focussed to a spot $\gtrsim 100\,\mu$m, for which it can provide an estimate for the accelerating wakefield and its dynamics, in synergy with massive PIC simulations, such as those of the UCLA group.[14,48] While the earlier (oversimplified!) analytical local models preferred very short (single oscillation) laser pulses, the stretching that was observed in our numerical solution implied that an optimized LPA system requires a longer pulse. Kinetic effects, e.g., plasma wave-breaking, trapping of resonant particles, and their subsequent acceleration, are not included in the present analysis. They are the subject of our study in progress that will be presented later.

ACKNOWLEDGMENTS

This work was supported in part by Grant No. 171006 of the Serbian Ministry of Science and Education. One of the authors (D.J.) acknowledges financial support from the fondo FAI of Italian INFN and a kind hospitality of Dipartimento di Fisica, Università di Napoli Federico II. Work at the Texas A&M University at Qatar is supported by the NPRP 6-021-1-005 project from the Qatar National Research Foundation (a member of the Qatar Foundation).

[1]M. N. Rosenbluth and C. S. Liu, Phys. Rev. Lett. **29**, 701 (1972).
[2]T. Tajima and J. M. Dawson, Phys. Rev. Lett. **43**, 267 (1979).
[3]L. M. Gorbunov and V. I. Kirsanov, Zh. Eksperimentalynoi Teor. Fiz. **93**, 509 (1987).
[4]P. Sprangle, E. Esarey, A. Ting, and G. Joyce, Appl. Phys. Lett. **53**, 2146 (1988).
[5]D. Jovanović, R. Fedele, F. Tanjia, S. De Nicola, and L. A. Gizzi, Eur. Phys. J. D **66**, 328 (2012).

[6]X. Wang, R. Zgadzaj, N. Fazel, Z. Li, S. A. Yi, X. Zhang, W. Henderson, Y.-Y. Chang, R. Korzekwa, H.-E. Tsai *et al.*, Nat. Commun. **4**, 1988 (2013).
[7]A. V. Korzhimanov, A. A. Gonoskov, E. A. Khazanov, and A. M. Sergeev, Phys. Usp. **54**, 9 (2011).
[8]O. Chekhlov, E. J. Divall, K. Ertel, S. J. Hawkes, C. J. Hooker, I. N. Ross, P. Matousek, C. Hernandez-Gomez, I. Musgrave, Y. Tang *et al.*, SPIE Conf. Ser. **6735**, 67350J (2007).
[9]D. Pepler, A. Boyle, J. Collier, M. Galimberti, C. Hernandez-Gomez, P. Holligan, A. Kidd, A. Lyachev, I. Musgrave, W. Shaikh *et al.*, in *Proceedings of ICALEPCS2009*, Kobe, Japan (2009), pp. 272–274.
[10]L. Pribyl, L. Juha, G. Korn, T. Levato, D. Margarone, B. Rus, S. Sebban, and S. Ter-Avetisyan, in *Proceedings of IBIC2012*, Tsukuba, Japan (2012), pp. 482–485.
[11]F. S. Tsung, C. Ren, L. O. Silva, W. B. Mori, and T. Katsouleas, Proc. Natl. Acad. Sci. U. S. A. **99**, 29–32 (2002).
[12]C. Ren, B. J. Duda, R. G. Hemker, W. B. Mori, T. Katsouleas, T. M. Antonsen, and P. Mora, Phys. Rev. E **63**, 026411 (2001).
[13]O. Shorokhov, A. Pukhov, and I. Kostyukov, Phys. Rev. Lett. **91**, 265002 (2003).
[14]W. Mori, W. An, V. K. Decyk, W. Lu, F. S. Tsung, R. A. Fonseca, S. F. Martins, J. Vieira, L. O. Silva, M. Chen *et al.*, in *Proceedings of Scientific Discovery Through Advanced Computing (SciDAC)*, Chattanooga, Tennessee, USA, 11–15 July (2010), pp. 261–276.
[15]L. A. Gizzi, M. P. Anania, G. Gatti, D. Giulietti, G. Grittani, M. Kando, M. Krus, L. Labate, T. Levato, Y. Oishi *et al.*, Nucl. Instrum. Methods Phys. Res. Sect. B **309**, 202–209 (2013).
[16]L. A. Gizzi, F. Anelli, C. Benedetti, C. A. Cecchetti, A. Clozza, G. Di Pirro, N. Drenska, R. Faccini, D. Giulietti, D. Filippetto *et al.*, Il Nuovo Cimento **32C**, 433 (2009).
[17]P. Sprangle, E. Esarey, and A. Ting, Phys. Rev. Lett. **64**, 2011 (1990).
[18]V. I. Berezhiani and S. M. Mahajan, Phys. Rev. Lett. **73**, 1837 (1994).
[19]A. Sharma, I. Kourakis, and P. K. Shukla, Phys. Rev. E **82**, 016402 (2010).
[20]L. M. Gorbunov, S. Y. Kalmykov, and P. Mora, Phys. Plasmas **12**, 033101 (2005).
[21]C. B. Schroeder, C. Benedetti, E. Esarey, and W. P. Leemans, Phys. Rev. Lett. **106**, 135002 (2011).
[22]I. Kostyukov and A. Pukhov, Phys. Plasmas **17**, 054704 (2010).
[23]A. Sharma and I. Kourakis, Plasma Phys. Controlled Fusion **52**, 065002 (2010).
[24]A. Sharma and I. Kourakis, Laser Part. Beams **28**, 479 (2010).
[25]A. Barbini, W. Baldeschi, M. Galimberti, A. Gamucci, A. Giulietti, L. Gizzi, P. Koester, L. Labate, A. Rossi, and P. Tomassini, See http://pcfas-ci.fisica.unimi.it/Pagine/Documenti/CDR_PLASMONX.pdf for parameters of the FLAME laser system (p. 15).
[26]C. de Martinis, S. Cialdi, I. Boscolo, M. Rome, A. L. Bacci, C. Maroli, M. Mauri, M. Cola, and R. Bonifacio, *Proceedings of the EPAC 2006*, Edinburgh, Scotland (2006), Paper No. WEPLS021.
[27]A. Giulietti, P. Tomassini, M. Galimberti, D. Giulietti, L. A. Gizzi, P. Koester, L. Labate, T. Ceccotti, P. D'Oliveira, T. Auguste *et al.*, Phys. Plasmas **13**, 093103 (2006).
[28]F. Broggi and L. Serafini, INFN Report No. SPARC-EBD-10/01, 2010.
[29]C. Benedetti, P. Londrillo, S. Rambaldi, G. Turchetti, R. Bonifacio, M. Castellano, A. Clozza, L. Cultrera, G. Di Pirro, A. Drago *et al.*, See http://www.lnf.infn.it/rapatt/2008/06/PLASMONX.pdf for plasma parameters in the simulations of multi GeV high-quality e-beams (section 4.5).
[30]L. A. Gizzi, A. Bacci, S. Betti, C. A. Cecchetti, M. Ferrario, A. Gamucci, A. Giulietti, D. Giulietti, P. Koester, L. Labate *et al.*, Eur. Phys. J. Spec. Top. **175**, 3 (2009).
[31]W. Lu, C. Huang, M. Zhou, M. Tzoufras, F. S. Tsung, W. B. Mori, and T. Katsouleas, Phys. Plasmas **13**, 056709 (2006).
[32]I. Kostyukov, A. Pukhov, and S. Kiselev, Phys. Plasmas **11**, 5256 (2004).
[33]A. Pukhov and J. Meyer-ter-Vehn, Appl. Phys. B: Lasers Opt. **74**, 355 (2002).
[34]E. Esarey, C. B. Schroeder, and W. P. Leemans, Rev. Modern Phys. **81**, 1229 (2009).
[35]S. Gordienko and A. Pukhov, Phys. Plasmas **12**, 043109 (2005).
[36]A. Pukhov and S. Gordienko, Philos. Trans. R. Soc., A **364**, 623 (2006).
[37]A. A. Balakin, A. G. Litvak, V. A. Mironov, and S. A. Skobelev, EPL (Europhys. Lett.) **100**, 34002 (2012).
[38]A. Pipahl, E. A. Anashkina, M. Toncian, T. Toncian, S. A. Skobelev, A. V. Bashinov, A. A. Gonoskov, O. Willi, and A. V. Kim, Phys. Rev. E **87**, 033104 (2013).
[39]A. Sharma, J. Borhanian, and I. Kourakis, J. Phys. A: Math. Gen. **42**, 465501 (2009).
[40]B. Cowan, D. Bruhwiler, E. Cormier-Michel, E. Esarey, C. G. R. Geddes, P. Messmer, and K. Paul, in *American Institute of Physics Conference Series*, edited by C. B. Schroeder, W. Leemans, and E. Esarey (AIP Publishing, 2009), Vol. 1086, pp. 309–314.
[41]D. Jovanovic and S. Vuković, Physica B+C **125**, 369 (1984).
[42]V. S. Belyaev, V. P. Krainov, V. S. Lisitsa, and A. P. Matafonov, Phys. Usp. **51**, 793 (2008).
[43]F. Pegoraro, S. V. Bulanov, F. Califano, and M. Lontano, Phys. Scr. **T63**, 262 (1996).
[44]G. A. Askar'yan, S. V. Bulanov, F. Pegoraro, and A. M. Pukhov, Plasma Phys. Rep. **21**, 835 (1995).
[45]D. Jovanović, F. Pegoraro, and F. Califano, Phys. Plasmas **8**, 3217 (2001).
[46]S. Y. Kalmykov, B. A. Shadwick, A. Beck, and E. Lefebvre, in *Proceeding of the InTech 2011 Femtosecond-Scale Optics*, Rijeka, Croatia, edited by A. V. Andreev (2011), pp. 113–138.
[47]B. M. Cowan, S. Y. Kalmykov, A. Beck, X. Davoine, K. Bunkers, A. F. Lifschitz, E. Lefebvre, D. L. Bruhwiler, B. A. Shadwick, and D. P. Umstadter, J. Plasma Phys. **78**, 469 (2012), 1204.0838.
[48]W. Lu, M. Tzoufras, C. Joshi, F. S. Tsung, W. B. Mori, J. Vieira, R. A. Fonseca, and L. O. Silva, Phys. Rev. Spec. Top. Accel. Beams **10**, 061301 (2007).